Research Square

Preprints are preliminary reports that have not undergone peer review.
They should not be considered conclusive, used to inform clinical practice,
or referenced by the media as validated information.

Fibronectin mediates bidirectional elasticity changes in cell-laden collagen scaffolds

Javad Eslami
University of Ottawa
Joshua D. Clugston
University of Ottawa
Fan Wan
University of Ottawa
Nadia Soulioti
University of Glasgow
Oana Dobre
University of Glasgow
James Harden
University of Ottawa
Delphine Gourdon
delphine.gourdon@glasgow.ac.uk

University of Glasgow

Article

Keywords: extracellular matrix, mechanobiology, collagen, fibronectin, cell-matrix interactions, viscoelasticity, 3D scaffolds, tissue engineering

Posted Date: November 6th, 2026

DOI: https://doi.org/10.21203/rs.3.rs-11138535/v1

License: This work is licensed under a Creative Commons Attribution 4.0 International License.
Read Full License

Additional Declarations: No competing interests reported.

Abstract

The extracellular matrix (ECM) provides cells with structural support and mechanical cues that regulate fundamental cellular processes. While ECM mechanics is known to influence cell behaviour, the reciprocal effect, how cells modify ECM mechanical properties, remains poorly understood, particularly in three-dimensional (3D) environments. Here, we engineered tuneable 3D collagen-fibronectin scaffolds with distinct microarchitectures (cold-cast: thick fibres, large pores; warm-cast: thin fibres, small pores) to investigate how embedded fibroblasts affect scaffold elasticity. We found that fibronectin is essential for cells to alter scaffold mechanics: in collagen-only scaffolds, cells induced structural changes but no mechanical change. Strikingly, in collagen-fibronectin scaffolds, cells softened cold-cast but stiffened warm-cast scaffolds, a bidirectional response demonstrating that cell-induced elasticity changes are critically dependent on matrix microarchitecture. Pair distribution function analysis showed that cells disrupt fibre connectivity in cold-cast scaffolds but preserve network organisation in warm-cast scaffolds, with implications for tissue engineering and disease.

Introduction

The mechanical properties of the extracellular matrix (ECM) are now recognised as fundamental regulators of cell behaviour, influencing processes ranging from stem cell differentiation to cancer progression[1–3]. Seminal work by Discher and colleagues demonstrated that matrix elasticity directs stem cell lineage specification, with soft matrices promoting neurogenic differentiation and stiff matrices favouring osteogenic fates[1]. In cancer, Weaver and colleagues showed that increased ECM stiffness promotes malignant behaviour through enhanced integrin signalling and focal adhesion assembly[2]. These findings have established the paradigm that cells sense and respond to the mechanical properties of their microenvironment through mechanotransduction pathways[3,4].

However, cell-ECM mechanical interactions are inherently bidirectional. Cells not only respond to ECM mechanics but also actively modify matrix properties through multiple mechanisms[5–7]. On longer timescales, cells remodel the ECM through synthesis and secretion of matrix proteins and enzymatic degradation via matrix metalloproteinases[5,6]. On shorter timescales, cells may also alter ECM mechanics through physical interactions with the fibrillar network, although the precise mechanisms and their dependence on matrix properties remain to be fully elucidated[7,8]. Understanding how cells influence ECM mechanical properties is therefore critical for both fundamental biology and the development of therapeutic strategies targeting the tumour microenvironment.

The native ECM is a complex three-dimensional (3D) network composed primarily of fibrous proteins, including collagens, fibronectin, elastin, and laminins, embedded in a hydrated proteoglycan-rich ground substance[9]. Collagen, particularly type I collagen, is the most abundant structural protein and provides the primary mechanical scaffold of most tissues[10]. Fibronectin is a key adhesive glycoprotein that mediates cell-matrix interactions through integrin binding, notably via its well-characterised RGD motif,

and independently associates with collagen fibres through multiple binding domains[11,12]. Fibronectin provides substantially more integrin binding sites than collagen, which may enable more effective mechanical coupling between cells and the matrix[13]. This difference in binding capacity makes fibronectin a critical component for studying how cells interact with and influence ECM mechanics[14].

The mechanical behaviour of ECM is inherently viscoelastic, exhibiting both elastic (energy-storing) and viscous (energy-dissipating) responses that are time- and rate-dependent[15]. ECM mechanics are determined by multiple factors including protein concentration, fibre architecture, crosslinking density, and hydration state[16,17]. Collagen networks exhibit strain-stiffening behaviour, becoming stiffer under applied deformation, which is thought to protect tissues from damage while enabling long-range force transmission[18]. Critically, the microstructure of the collagen network, including fibre diameter, length, pore size, and connectivity, profoundly influences bulk mechanical properties and cellular mechanosensing[19,20].

While considerable progress has been made in understanding how ECM mechanics regulate cell behaviour in two-dimensional culture systems, cells *in vivo* reside within 3D microenvironments that present fundamentally different mechanical and topographical cues[21]. 3D culture systems are therefore essential for recapitulating physiologically relevant cell-ECM interactions. However, studying cell-induced mechanical changes in 3D presents significant technical challenges, as it requires scaffolds with controlled and tuneable properties, the ability to maintain long-term cultures, and methods to quantify both structural and mechanical changes[22].

Temperature-mediated casting provides an effective approach to fabricate tuneable collagen scaffolds with controlled microarchitecture[23]. By manipulating the temperature during gelation, the kinetics of collagen fibrillogenesis can be controlled: slower polymerisation at lower temperatures produces thicker fibres and larger pores, while rapid polymerisation at higher temperatures yields thinner fibres and smaller pores[24]. These porous collagen scaffolds provide excellent substrates for protein adsorption, enabling the incorporation of fibronectin to create ECM-mimicking platforms that support long-term 3D cell culture in physiologically relevant volumes[23].

In this study, we systematically investigate how embedded cells affect the mechanical properties of 3D collagen-based scaffolds as a function of matrix composition and microarchitecture. We fabricated collagen and collagen-fibronectin scaffolds with two distinct microarchitectures using temperature-mediated casting, characterised their structural and viscoelastic properties, and examined how embedded fibroblasts modulate these properties. Our findings reveal that fibronectin is essential for cell-mediated mechanical changes, and that scaffold microarchitecture determines whether this effect manifests as stiffening or softening. These results provide new insights into the bidirectional nature of cell-ECM mechanical interactions and have implications for tissue engineering, disease modelling, and our fundamental understanding of mechanobiology.

Results

Temperature-mediated casting produces fibrillar scaffolds with distinct microarchitectures

We fabricated 3D collagen scaffolds using a temperature-mediated casting approach that exploits the temperature-dependence of collagen fibrillogenesis kinetics (Fig. 1). In the cold-casting protocol, neutralised collagen solutions were gradually polymerised through a temperature ramp from 4°C to 37°C, producing scaffolds with thick fibres (diameter: 3.4 ± 0.3 μm) and large pores (area: 2542 ± 1375 μm^2). In contrast, warm-casting involved rapid polymerisation at 37°C, yielding scaffolds with thinner fibres (diameter: 2.3 ± 0.2 μm, $p < 0.001$ vs. cold-cast) and slightly smaller pores (area: 2289 ± 821 μm^2, $p < 0.01$ vs. cold-cast). Fibre length was also significantly greater in cold-cast scaffolds (52.9 ± 7.9 μm) compared to warm-cast scaffolds (38.1 ± 4.3 μm, $p < 0.001$).

Despite these substantial microstructural differences, rheological characterisation revealed that the bulk elastic properties of the two scaffold types were similar. The storage modulus (G') at 0.1% strain amplitude and 10 rad/s was 842 ± 211 Pa for cold-cast scaffolds and 604 ± 313 Pa for warm-cast scaffolds ($n = 4$, $p = 0.4946$ no statistical significance). This result indicates that the temperature-mediated casting approach enables independent control of scaffold microarchitecture without substantially altering bulk stiffness, providing an ideal platform to investigate how microstructural features influence the mechanical effects of embedded cells.

Cells alter collagen scaffold structure but not bulk mechanics in the absence of fibronectin

To investigate how cells affect scaffold properties, we embedded GFP-expressing NIH/3T3 fibroblasts within collagen scaffolds at a seeding density of 1.3×10^5 cells/mL and cultured them for 24 hours before analysis (Fig. 1d–f, j–l). Confocal microscopy revealed that cells induced measurable structural changes: fibre diameter decreased from 3.4 ± 0.3 μm to 3.0 ± 0.3 μm in cold-cast scaffolds ($p < 0.05$) and from 2.3 ± 0.2 μm to 2 ± 0.2 μm in warm-cast scaffolds ($p < 0.01$). Similarly, fibre length decreased significantly in both scaffold types upon cell incorporation (cold-cast: from 52.9 ± 7.9 μm to 36.5 ± 4.8 μm, $p < 0.001$; warm-cast: from 38.2 ± 4.3 μm to 29.9 ± 3.7 μm, $p < 0.001$).

Despite these structural changes, rheological measurements revealed no significant differences in storage modulus between cell-free and cell-laden collagen scaffolds for either casting condition (Fig. 1p). The storage modulus of cell-laden cold-cast scaffolds (704 ± 120 Pa) was comparable to cell-free controls (842 ± 211 Pa), and similarly, cell-laden warm-cast scaffolds (909 ± 154 Pa) showed no significant change from cell-free warm-cast scaffolds (604 ± 313 Pa). These findings indicate that while cells induce local structural reorganisation, these changes are insufficient to alter the bulk mechanical properties of the scaffolds in the absence of fibronectin.

Fibronectin incorporation alters scaffold structure and increases scaffold stiffness

We next examined the effects of incorporating fibronectin into the collagen scaffolds (Fig. 2). Fibronectin was added to the collagen solution prior to gelation at a final concentration of 0.2 mg/mL. Confocal microscopy revealed that fibronectin incorporation significantly affected scaffold microstructure in both cold-cast and warm-cast systems. In cold-cast scaffolds, fibre diameter decreased from 3.4 ± 0.3 μm (collagen only) to 2.6 ± 0.3 μm (collagen-fibronectin, $p < 0.001$), and pore size decreased from 2542 ± 1375 μm^2 to 1453 ± 445 μm^2 ($p < 0.01$). Similar trends were observed in warm-cast scaffolds, with fibronectin reducing fibre diameter to 1.6 ± 0.1 μm ($p < 0.001$ vs. collagen only) and pore size to 593 ± 166 μm^2 ($p < 0.001$ vs. collagen only).

These structural changes were accompanied by increased scaffold stiffness. The addition of fibronectin increased the storage modulus of cold-cast scaffolds from 842 ± 211 Pa to 918 ± 176 Pa, and more substantially increased the modulus of warm-cast scaffolds from 604 ± 313 Pa to 1150.0 ± 97 Pa ($p < 0.05$ vs. collagen-only warm-cast). The greater stiffening effect in warm-cast scaffolds likely reflects their smaller pore sizes and increased fibre interconnectivity, which amplify the mechanical contribution of fibronectin-mediated crosslinks.

Fibronectin enables bidirectional cell-induced elasticity changes

Having established that cells alone do not alter the bulk mechanics of collagen scaffolds and that fibronectin modifies scaffold structure and stiffness, we investigated whether fibronectin enables cell-mediated mechanical effects (Figs. 3 and 4). Strikingly, in the presence of fibronectin, cells exerted significant and opposing effects on scaffold mechanics depending on the microarchitecture.

In cold-cast collagen-fibronectin scaffolds, the addition of cells resulted in decreased mechanical stiffness: the storage modulus dropped from 918 ± 176 Pa (cell-free) to 361 ± 61 Pa (cell-laden, $p < 0.01$, Fig. 3p). In contrast, in warm-cast collagen-fibronectin scaffolds, cells induced mechanical stiffening: the storage modulus increased from 1150 ± 97 Pa (cell-free) to 1608 ± 280 Pa (cell-laden, $p < 0.05$, Fig. 4p). This bidirectional mechanical response represents a key finding of this study: cells soften cold-cast but stiffen warm-cast scaffolds, demonstrating that the effect of embedded cells on scaffold elasticity is critically dependent on matrix microarchitecture.

Microstructural analysis revealed that in cell-laden collagen-fibronectin scaffolds, fibre dimensions were comparable between cold-cast and warm-cast conditions (fibre diameter: 2.63 ± 0.3 μm vs. 1.70 ± 0.1 μm; fibre length: 38.9 ± 6.7 μm vs. 27.4 ± 4.1 μm). However, pore size differed substantially: cold-cast scaffolds retained larger pores (1546 ± 519 μm^2) compared to warm-cast scaffolds (539 ± 115 μm^2), though both were significantly reduced compared to their respective collagen-only controls. These observations suggest that the divergent mechanical outcomes are not simply explained by differences in

final microstructure but rather reflect differences in how cells interact with the two scaffold architectures.

Pair distribution function analysis reveals distinct patterns of structural change

To gain deeper insight into the structural basis for the opposing mechanical effects, we performed pair distribution function (PDF) analysis on confocal images of cell-laden collagen-fibronectin scaffolds (Fig. 5). Representative stacked confocal images used for the analysis are shown for cold-cast (Fig. 5a) and warm-cast (Fig. 5b) cell-laden scaffolds. The PDF quantifies the probability of finding pairs of fibres at given separation distances relative to a random distribution, providing information about network connectivity and organisation (see Supplementary Methods).

Comparison of the PDF profiles for the cell-laden cold-cast and warm-cast scaffolds (Fig. 5c) revealed fundamentally different fibre organisation patterns between the two scaffold types. In warm-cast scaffolds, the PDF decreased approximately linearly with increasing separation distance, consistent with a relatively uniform fibre distribution and maintained network connectivity. In contrast, cold-cast scaffolds exhibited a biphasic decay in the PDF, indicating reduced fibre connectivity and more heterogeneous fibre distribution. This pattern suggests that cells in cold-cast scaffolds locally disrupt the fibre network, creating regions of altered fibre density, which would reduce load-bearing capacity and explain the observed softening.

Further PDF analysis comparing scaffolds with and without cells revealed how cells differentially affect network structure depending on microarchitecture (Fig. 5d,e). In warm-cast scaffolds, the PDF curves for cell-free and cell-laden samples largely overlapped, indicating that cells have minimal effect on fibre spatial distribution. In contrast, in cold-cast scaffolds, cell incorporation substantially altered the PDF, with cell-laden samples showing reduced connectivity compared to cell-free controls. Together, these structural analyses provide a framework for understanding the bidirectional mechanical response: in cold-cast scaffolds, cells disrupt network connectivity and reduce stiffness, whereas in warm-cast scaffolds, cells exert more uniform effects that preserve network organisation while enabling matrix compaction and stiffening.

Discussion

In this study, we demonstrate that embedded cells can induce either stiffening or softening of 3D collagen-based scaffolds depending on the presence of fibronectin and the scaffold microarchitecture. This bidirectional elasticity response has important implications for our understanding of cell-ECM mechanical interplay and the design of biomaterials for tissue engineering and disease modelling.

A central observation of this work is that fibronectin is required for cells to affect bulk scaffold mechanics. In collagen-only scaffolds, cells induced measurable structural changes, i.e., reducing fibre

diameter and length, yet these changes did not translate into altered bulk mechanical properties. One plausible interpretation is that this reflects differences in cell-matrix interaction strength: fibronectin provides abundant integrin binding sites (particularly RGD motifs recognised by $\alpha_5\beta_1$ and $\alpha_v\beta_3$ integrins), whereas type I collagen offers fewer high-affinity integrin binding sites (primarily for $\alpha_1\beta_1$ and $\alpha_2\beta_1$)[25,26]. If cells interact more strongly with fibronectin-containing matrices, they may be better able to transmit forces to the surrounding network and thereby influence bulk mechanical properties. However, we note that this interpretation remains a hypothesis, as we did not directly quantify cell-matrix adhesion in this study. Future work examining focal adhesion formation, integrin expression, or cell-generated traction forces would be needed to test this mechanism directly.

The opposing mechanical effects of cells in cold-cast versus warm-cast scaffolds highlight the critical role of microarchitecture in determining the outcome of cell-ECM interactions. Several factors may contribute to this divergence. First, the larger pore sizes in cold-cast scaffolds allow cells greater freedom to spread and extend cellular processes. When cells contract, they may exert localised forces that pull fibres together in some regions while creating voids elsewhere, leading to a more heterogeneous network structure. This interpretation is consistent with our PDF analysis showing reduced fibre connectivity in cell-laden cold-cast scaffolds. In contrast, the smaller pores of warm-cast scaffolds constrain cell spreading, potentially resulting in more uniform force distribution that compacts rather than disrupts the matrix. This would be consistent with previous work showing that cell spreading and force generation are sensitive to matrix pore size and stiffness[27,28].

Second, the connectivity and percolation characteristics of the two scaffold types may differ. Cold-cast scaffolds, with their thick but sparse fibres, may represent marginally percolating networks that are more susceptible to disruption by local perturbations. If cells locally displace or bundle fibres, they could compromise network connectivity and reduce the number of load-bearing pathways through the scaffold. Warm-cast scaffolds, with their denser fibre networks, may be more robust to local perturbations and better able to maintain mechanical integrity when cells are incorporated[29].

An alternative but not mutually exclusive interpretation is that cells physically bridge fibres within the network, effectively acting as additional structural elements. In this view, the outcome would depend on whether cell-mediated bridging enhances or disrupts load transfer. In the dense warm-cast networks, cells connecting nearby fibres could reinforce the existing structure. In the sparse cold-cast networks, cells attempting to bridge distant fibres might instead pull fibres out of their load-bearing configurations. While this interpretation is consistent with our observations and with the requirement for fibronectin (which would enhance cell-fibre coupling), it remains speculative without direct measurements of cell-matrix connections or force transmission.

Our findings extend previous work on cell-ECM mechanical interactions by demonstrating that the mechanical outcome is not simply a function of cell activity but depends critically on the structural context. Prior studies have reported both cell-induced stiffening and softening of collagen matrices[30,31], and our results suggest that these apparently contradictory findings may reflect differences in matrix

architecture rather than cell type or culture conditions. The concept that network architecture determines whether cells stiffen or soften the matrix has important implications for interpreting mechanical measurements of cell-populated matrices and for designing biomaterials with predictable mechanical responses to cellular incorporation.

From a mechanobiology perspective, the bidirectional elasticity response we observe may have physiological relevance. In tissues, ECM architecture varies substantially between different anatomical locations and developmental stages. The ability of cells to produce opposite mechanical effects depending on local architecture suggests that tissue mechanics could be fine-tuned through matrix structural organisation, independent of matrix composition or cell contractility. Conversely, disruptions to this balance, either through altered ECM composition or architecture, may contribute to pathological stiffening or softening observed in diseases such as fibrosis and cancer[32,33].

For tissue engineering applications, our results highlight the importance of considering both matrix composition and architecture when designing scaffolds for cell-based therapies. The ability to independently tune microarchitecture (through casting temperature) and composition (through fibronectin incorporation) provides a versatile platform for creating scaffolds with defined structure-mechanics relationships. Furthermore, understanding how cells will affect scaffold mechanics is essential for predicting their long-term mechanical performance in vivo.

Some aspects of our study point to questions that remain open. We used a single cell type (NIH/3T3 fibroblasts) at a single seeding density, and different cell types or densities may produce different outcomes. Our mechanical measurements were also performed at a single time point (24 hours), which captures relatively early cell-matrix interactions; longer-term studies would be needed to assess how these effects evolve as cells begin to deposit or degrade matrix components. Most importantly, while our PDF analysis provides structural insights, we did not directly characterise cell-matrix adhesions (for example, through immunostaining for focal adhesion proteins or analysis of integrin expression) or measure cell-generated forces and their spatial distribution. Although the fibronectin-dependence of the mechanical effects strongly suggests a role for enhanced cell-matrix interactions, the precise mechanism remains to be determined. Techniques such as traction force microscopy adapted for 3D systems[34], adhesion complex imaging, or integrin-blocking experiments would help to address these questions and directly test the proposed mechanism.

Taken together, our results demonstrate that the presence of cells can induce bidirectional elasticity changes in 3D collagen-fibronectin scaffolds, with fibronectin enabling and microarchitecture determining the direction of these effects. The fibronectin-dependence suggests that cell-matrix interactions play a key role, although the precise mechanisms await further investigation. These findings provide new insights into the bidirectional nature of cell-ECM mechanical interplay and have implications for understanding tissue homeostasis, disease progression, and the rational design of biomaterials for regenerative medicine.

Methods

Fabrication of 3D collagen and collagen-fibronectin scaffolds

Scaffolds were fabricated from type I collagen microfibrils derived from rat tail (Advanced BioMatrix, San Diego, CA, USA) at a stock concentration of 4.1 mg/mL and bovine plasma fibronectin (Invitrogen, Thermo Fisher Scientific, Waltham, MA, USA) at 1 mg/mL. Neutralised collagen solution was prepared by mixing the acidic collagen stock with neutralisation solution (Advanced BioMatrix) at a 9:1 ratio. For collagen-only scaffolds, 280 µL of neutralised collagen solution was combined with 70 µL PBS and added to custom moulds (12 × 12 × 3 mm^3). For collagen-fibronectin scaffolds, 70 µL of fibronectin solution was added to 280 µL of neutralised collagen solution, yielding final concentrations of 2.9 mg/mL collagen and 0.2 mg/mL fibronectin.

Two casting protocols were employed to generate scaffolds with distinct microarchitectures. For cold-cast scaffolds, solutions were added to pre-cooled moulds at 4°C and polymerised through a gradual temperature ramp: 4°C for 15 minutes (refrigerator), 15°C for 15 minutes (environmental chamber), followed by 37°C with 5% CO_2 for 24 hours (incubator). For warm-cast scaffolds, solutions were added to pre-warmed moulds at 15°C and rapidly polymerised at 37°C with 5% CO_2. Following gelation, 150 µL of cell culture medium was added to each scaffold.

Cell culture and scaffold seeding

GFP-expressing NIH/3T3 fibroblasts (GFP-3T3) were cultured in Dulbecco's Modified Eagle Medium (D-MEM; Sigma-Aldrich, St. Louis, MO, USA) supplemented with 10% (v/v) foetal bovine serum (FBS; Tissue Culture Biologics) and 1% (v/v) penicillin/streptomycin (Life Technologies) at 37°C in a humidified atmosphere with 5% CO_2. For cell-laden scaffolds, cells were mixed with the collagen (or collagen-fibronectin) solution prior to casting at a seeding density of 1.3×10^5 cells/mL. To ensure homogeneous cell distribution, scaffolds were flipped every 15 minutes for 2 hours at 27°C after the initial 1-hour incubation, then incubated for a further 21 hours at 37°C with 5% CO_2 before analysis.

Confocal microscopy and structural analysis

Scaffolds were fixed in 4% formalin (Sigma-Aldrich) in phosphate-buffered saline (PBS; Life Technologies) for 20 minutes prior to imaging. Confocal fluorescence microscopy was performed using a Zeiss LSM880 laser scanning microscope (Zeiss, Oberkochen, Germany) equipped with a 20× objective. For each sample, fifteen random regions of interest (ROIs), each measuring 200 µm × 200 µm and sampled from different lateral positions and z-layers, were examined. Collagen was visualised by confocal reflectance microscopy; fibronectin and GFP-expressing cells were imaged by fluorescence.

Image analysis was performed using custom Python scripts together with manual measurements acquired in ZEN Blue (Zeiss). Fibre detection in Python was based on grayscale conversion, Gaussian

smoothing, Otsu-guided thresholding, and morphological cleaning (opening and closing) to obtain binarised fibre masks. Contours were identified using cv2.findContours, and each fibre-containing region was characterised by its centroid, convex hull, and fitted ellipse orientation. Fibre sub-segmentation was performed by generating radial line elements from each contour centroid toward its convex-hull vertices and placing evenly spaced circular sampling points along each line. These sampling points were used to approximate the spatial distribution of fibres for subsequent pairwise-distance and PDF-type analyses, as detailed in Supplementary Methods.

Quantification of fibre thickness, fibre length, and pore size was performed manually in ZEN Blue. For each condition, three independent samples were analysed. In each sample, fifteen randomly selected regions of interest (ROIs), each measuring 200 µm × 200 µm and sampled from different lateral positions and z-layers, were examined. Within each ROI, all individual measurements of fibre diameter and fibre length were collected using ZEN's line-profile tool; the mean of these thirty measurements was recorded for that ROI. The fifteen ROI means were then averaged to obtain the reported fibre thickness and length for each sample. Pore size was measured using the same ROI-sampling strategy; however, because pore density varied across samples, between five and fifteen pores were measured per ROI, and the corresponding means were computed in an identical manner.

Rheological characterisation

Viscoelastic properties of scaffolds were measured using an MCR301 parallel plate rheometer (Anton Paar, Graz, Austria) equipped with 12 mm diameter circular plates matching the scaffold diameter. To prevent slippage, plate surfaces were sandblasted and scaffolds were secured using Permabond Instant Adhesive 102 (Permabond, Pottstown, PA, USA). Measurements were performed at room temperature (23–24°C) with a deionised water reservoir maintained at the sample periphery to prevent dehydration.

Oscillatory strain sweep measurements were performed to determine the linear viscoelastic region. Storage modulus values were then reported at a strain amplitude of 0.1% and an angular frequency of 10 rad/s, a condition within the linear viscoelastic regime for all samples.Four independent samples were tested for each condition. Data were analysed using custom Python scripts and GraphPad Prism.

Statistical analysis

Statistical analyses were performed using GraphPad Prism (GraphPad Software, San Diego, CA, USA). Data are displayed as box plots, with the box indicating the median and interquartile range, whiskers indicating the range, and + denoting the mean. Comparisons among multiple groups were made using one-way ANOVA with Tukey's post-hoc test for multiple comparisons. Statistical significance was defined as $p < 0.05$ and is indicated as follows: *$p < 0.05$, **$p < 0.01$, ***$p < 0.001$, ****$p < 0.0001$. Sample sizes (n) are indicated in figure legends.

Data Availability

The datasets generated and analysed during this study are available from the corresponding authors upon reasonable request.

Code Availability

The custom Python code used for image analysis in this study is provided as Supplementary Code. Full implementation details of the image analysis procedure are provided in the Supplementary Methods.

Declarations

Competing Interests

The authors declare that they have no competing financial interests or personal relationships that could have appeared to influence the work reported in this paper.

Author Contribution

J.E. designed and performed experiments, analysed data, and wrote the manuscript. J.D.C. trained J.E. for rheology experiments. F.W. contributed cell culture and immunostaining. N.S. and O.D. critically reviewed the manuscript, data, and figures. J.H. and D.G. conceived the study, supervised the project, and revised the manuscript. All authors read and approved the final manuscript.

Acknowledgement

J.E., J.D.C., F.W. and JH acknowledge funding from the Canadian National Science and Engineering Research Council through Discovery Grant RGPIN-2024-06902. J.E. was also supported in part by the Graduate Division of the University of Ottawa, Canada. N.S. and D.G. acknowledge the British Royal Society under the Wolfson award RSWF/FT/191020. The funders had no role in study design, data collection, analysis, interpretation, or manuscript preparation.

Data Availability

Data Availability: The datasets generated and analysed during this study are available from the corresponding authors upon reasonable request.Code Availability: The custom Python code used for image analysis in this study is provided as Supplementary Code. Full implementation details of the image analysis procedure are provided in the Supplementary Methods.

References

1. Engler, A. J., Sen, S., Sweeney, H. L. & Discher, D. E. Matrix elasticity directs stem cell lineage specification. *Cell* 126, 677–689 (2006).

2. Paszek, M. J. *et al.* Tensional homeostasis and the malignant phenotype. *Cancer Cell* 8, 241–254 (2005).
3. Humphrey, J. D., Dufresne, E. R. & Schwartz, M. A. Mechanotransduction and extracellular matrix homeostasis. *Nat. Rev. Mol. Cell Biol.* 15, 802–812 (2014).
4. Vogel, V. & Sheetz, M. Local force and geometry sensing regulate cell functions. *Nat. Rev. Mol. Cell Biol.* 7, 265–275 (2006).
5. Lu, P., Weaver, V. M. & Werb, Z. The extracellular matrix: a dynamic niche in cancer progression. *J. Cell Biol.* 196, 395–406 (2012).
6. Lu, P., Takai, K., Weaver, V. M. & Werb, Z. Extracellular matrix degradation and remodeling in development and disease. *Cold Spring Harb. Perspect. Biol.* 3, a005058 (2011).
7. Bonnans, C., Chou, J. & Bhowmick, N. A. Remodelling the extracellular matrix in development and disease. *Nat. Rev. Mol. Cell Biol.* 15, 786–801 (2014).
8. Wang, H., Abhilash, A. S., Chen, C. S., Wells, R. G. & Shenoy, V. B. Long-range force transmission in fibrous matrices enabled by tension-driven alignment of fibers. *Biophys. J.* 107, 2592–2603 (2014).
9. Frantz, C., Stewart, K. M. & Weaver, V. M. The extracellular matrix at a glance. *J. Cell Sci.* 123, 4195–4200 (2010).
10. Lee, C. H., Singla, A. & Lee, Y. Biomedical applications of collagen. *Int. J. Pharm.* 221, 1–22 (2001).
11. Kubow, K. E. *et al.* Mechanical forces regulate the interactions of fibronectin and collagen I in extracellular matrix. *Nat. Commun.* 6, 8026 (2015).
12. Smith, M. L. *et al.* Force-induced unfolding of fibronectin in the extracellular matrix of living cells. *PLoS Biol.* 5, e268 (2007).
13. Schwarzbauer, J. E. & DeSimone, D. W. Fibronectins, their fibrillogenesis, and in vivo functions. *Cold Spring Harb. Perspect. Biol.* 3, a005041 (2011).
14. Dallas, S. L., Chen, Q. & Sivakumar, P. Dynamics of assembly and reorganization of extracellular matrix proteins. *Curr. Top. Dev. Biol.* 75, 1–24 (2006).
15. Chaudhuri, O., Cooper-White, J., Bhave, M., Janmey, P. A. & Bhardwaj, R. S. Hydrogels with tunable stress relaxation regulate stem cell fate and activity. *Nat. Mater.* 15, 326–334 (2016).
16. Ge, H., Tian, M., Pei, Q., Tan, F. & Pei, H. Extracellular matrix stiffness: new areas affecting cell metabolism. *Front. Oncol.* 11, 631991 (2021).
17. Deng, B. *et al.* Biological role of matrix stiffness in tumor growth and treatment. *J. Transl. Med.* 20, 540 (2022).
18. Storm, C., Pastore, J. J., MacKintosh, F. C., Lubensky, T. C. & Janmey, P. A. Nonlinear elasticity in biological gels. *Nature* 435, 191–194 (2005).
19. Raub, C. B. *et al.* Noninvasive assessment of collagen gel microstructure and mechanics using multiphoton microscopy. *Biophys. J.* 92, 2212–2222 (2007).
20. Asadishekari, M. *et al.* Three-dimensional tunable fibronectin-collagen platforms for control of cell adhesion and matrix deposition. *Front. Phys.* 10, 806554 (2022).

21. Baker, B. M. & Chen, C. S. Deconstructing the third dimension – how 3D culture microenvironments alter cellular cues. *J. Cell Sci.* 125, 3015–3024 (2012).
22. Caliari, S. R. & Burdick, J. A. A practical guide to hydrogels for cell culture. *Nat. Methods* 13, 405–414 (2016).
23. Seo, B. R. *et al*. Collagen microarchitecture mechanically controls myofibroblast differentiation. *Proc. Natl. Acad. Sci. U.S.A.* 117, 11387–11398 (2020).
24. Raghunath, J. *et al.* Biomaterials and scaffold design: key to tissue-engineering cartilage. *Biotechnol. Appl. Biochem.* 46, 73–84 (2007).
25. Barczyk, M., Carracedo, S. & Gullberg, D. Integrins. *Cell Tissue Res.* 339, 269–280 (2010).
26. Hynes, R. O. Integrins: bidirectional, allosteric signaling machines. *Cell* 110, 673–687 (2002).
27. Gribova, V., Crouzier, T. & Picart, C. A material's point of view on recent developments of polymeric biomaterials: control of mechanical and biochemical properties. *J. Mater. Chem.* 21, 14354–14366 (2011).
28. Smith, L. R., Cho, S. & Discher, D. E. Stem cell differentiation is regulated by extracellular matrix mechanics. *Physiology* 33, 16–25 (2018).
29. Broedersz, C. P. & MacKintosh, F. C. Modeling semiflexible polymer networks. *Rev. Mod. Phys.* 86, 995–1036 (2014).
30. Winer, J. P., Oake, S. & Bhardwaj, R. S. Non-linear elasticity of extracellular matrices enables contractile cells to communicate local position and orientation. *PLoS ONE* 4, e6382 (2009).
31. Hall, M. S. *et al.* Fibrous nonlinear elasticity enables positive mechanical feedback between cells and ECMs. *Proc. Natl. Acad. Sci. USA* 113, 14043–14048 (2016).
32. Cox, T. R. & Erler, J. T. Remodeling and homeostasis of the extracellular matrix: implications for fibrotic diseases and cancer. *Dis. Model. Mech.* 4, 165–178 (2011).
33. Burgess, J. K., Mauad, T., Tjin, G., Karlsson, J. C. & Westergren-Thorsson, G. The extracellular matrix – the under-recognized element in lung disease? *J. Pathol.* 240, 397–409 (2016).
34. Legant, W. R. *et al.* Measurement of mechanical tractions exerted by cells in three-dimensional matrices. *Nat. Methods* 7, 969–971 (2010).

Figures

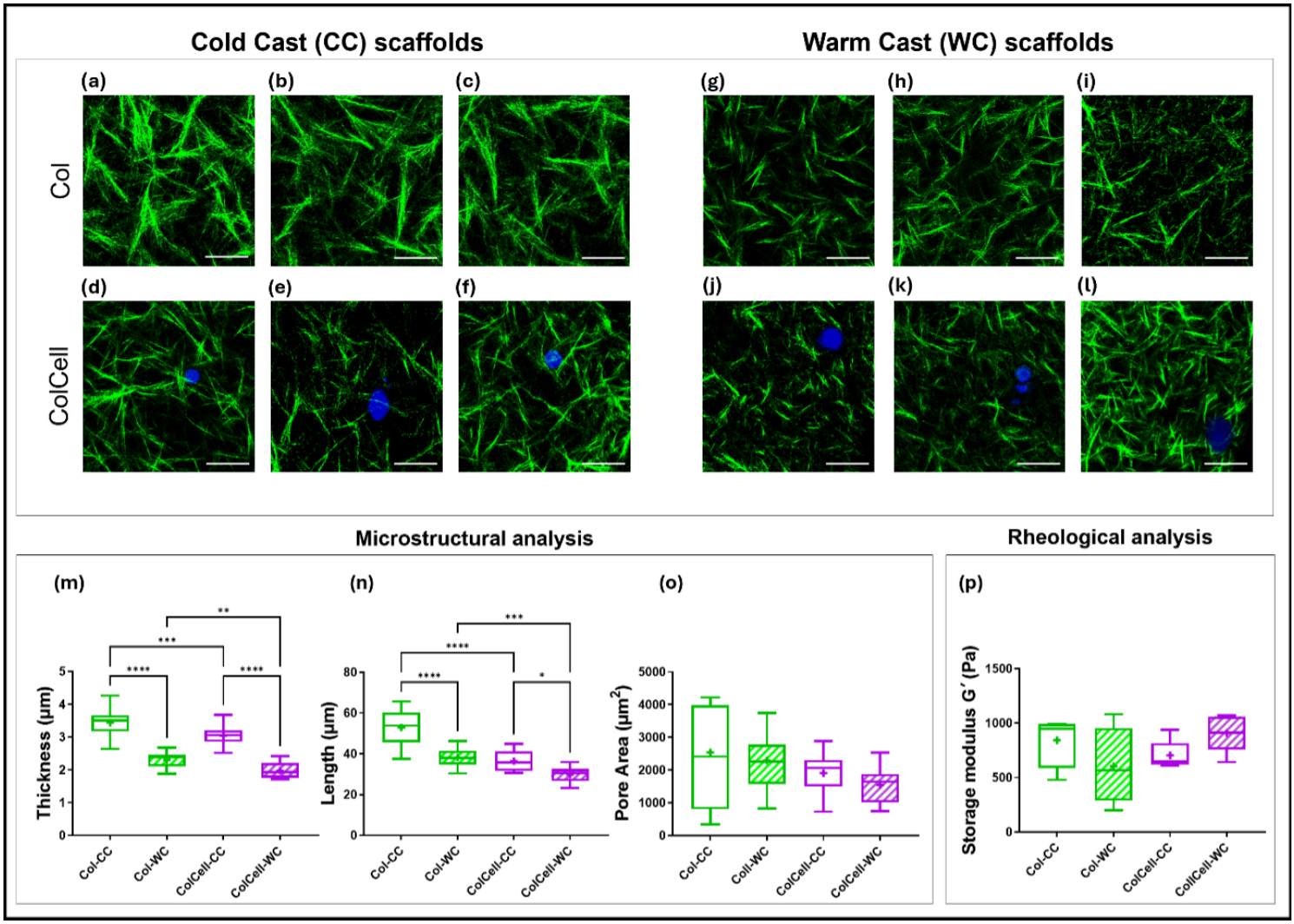


Figure 1

Microstructure and elastic properties of collagen scaffolds fabricated by temperature-mediated casting. (a–c) Representative confocal reflectance micrographs of cell-free cold-cast collagen scaffolds showing thick fibres and large pores characteristic of slow polymerisation. (d–f) Cold-cast collagen scaffolds containing embedded GFP-3T3 fibroblasts (green: collagen reflectance). (g–i) Warm-cast collagen scaffolds displaying thinner fibres and smaller pores resulting from rapid polymerisation. (j–l) Warm-cast collagen scaffolds with embedded cells. Scale bars: 50 µm. (m) Collagen fibre diameter. (n) Collagen fibre length. (o) Pore/mesh area. (p) Storage modulus (G') showing that cells do not significantly alter bulk scaffold elasticity in the absence of fibronectin. Rheological measurements performed at 0.1% strain amplitude and angular frequency of 10 rad/s. Data are presented as mean ± SD; n = 15 regions of interest from 3 independent scaffolds for structural analyses, n = 4 independent scaffolds for rheological measurements. Statistical comparisons by one-way ANOVA with Tukey's post-hoc test; *$p < 0.05$, **$p < 0.01$, ***$p < 0.001$, ****$p < 0.0001$.

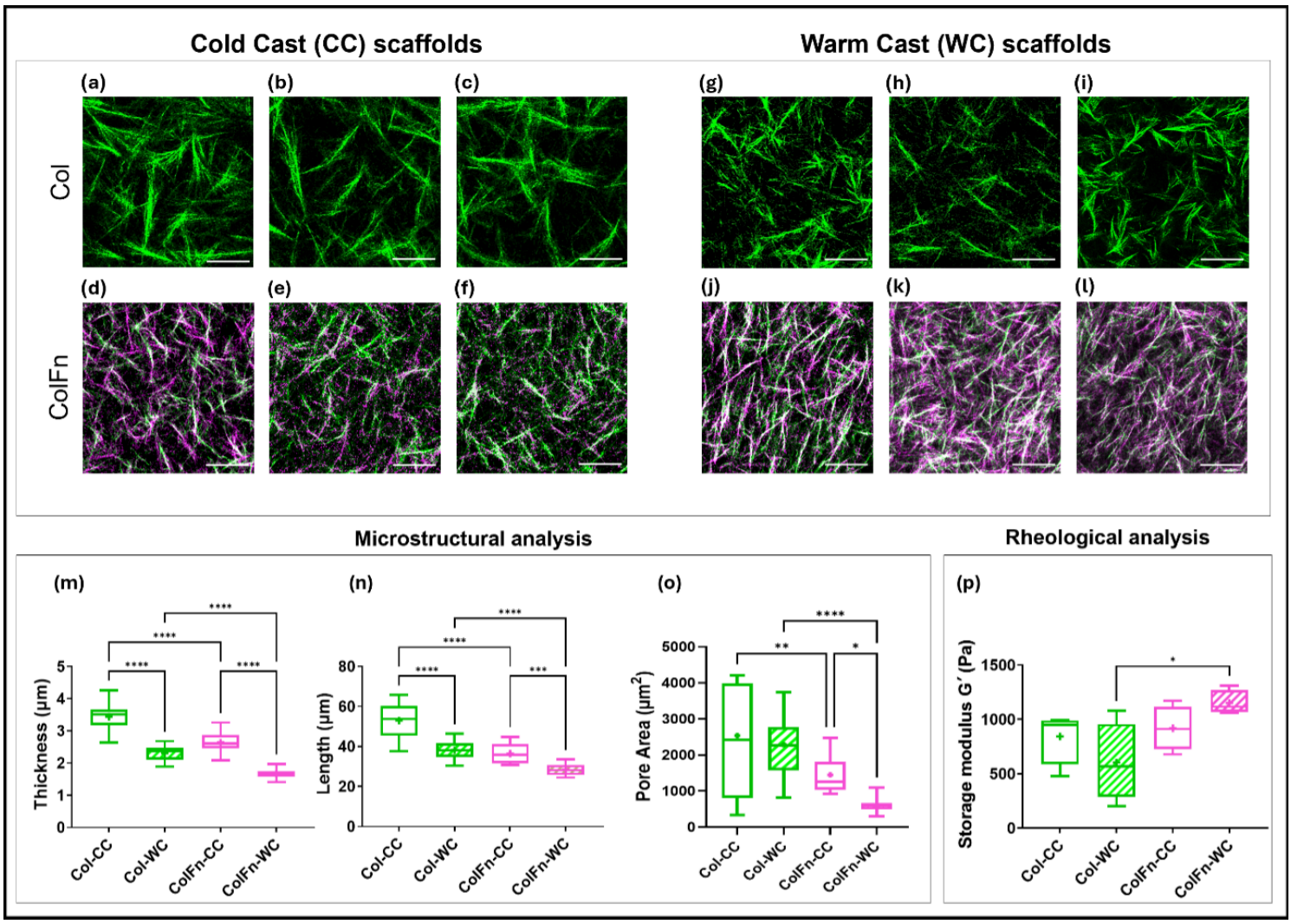


Figure 2

Fibronectin incorporation modifies collagen scaffold microstructure and increases stiffness. (a–c) Cold-cast collagen-only scaffolds (control). (d–f) Cold-cast collagen-fibronectin scaffolds showing reduced fibre dimensions and pore size (green: collagen reflectance; magenta: fibronectin fluorescence). (g–i) Warm-cast collagen-only scaffolds (control). (j–l) Warm-cast collagen-fibronectin scaffolds demonstrating the most compact microstructure. Scale bars: 50 µm. (m) Fibre diameter comparison. (n) Fibre length comparison. (o) Pore/mesh area comparison. (p) Storage modulus showing that fibronectin incorporation increases scaffold stiffness, with a more pronounced effect in warm-cast scaffolds. Data are presented as mean ± SD; n = 15 for structural analyses, n = 4 for rheological measurements. Statistical comparisons by one-way ANOVA with Tukey's post-hoc test; *$p < 0.05$, **$p < 0.01$, ***$p< 0.001$, ****$p < 0.0001$.

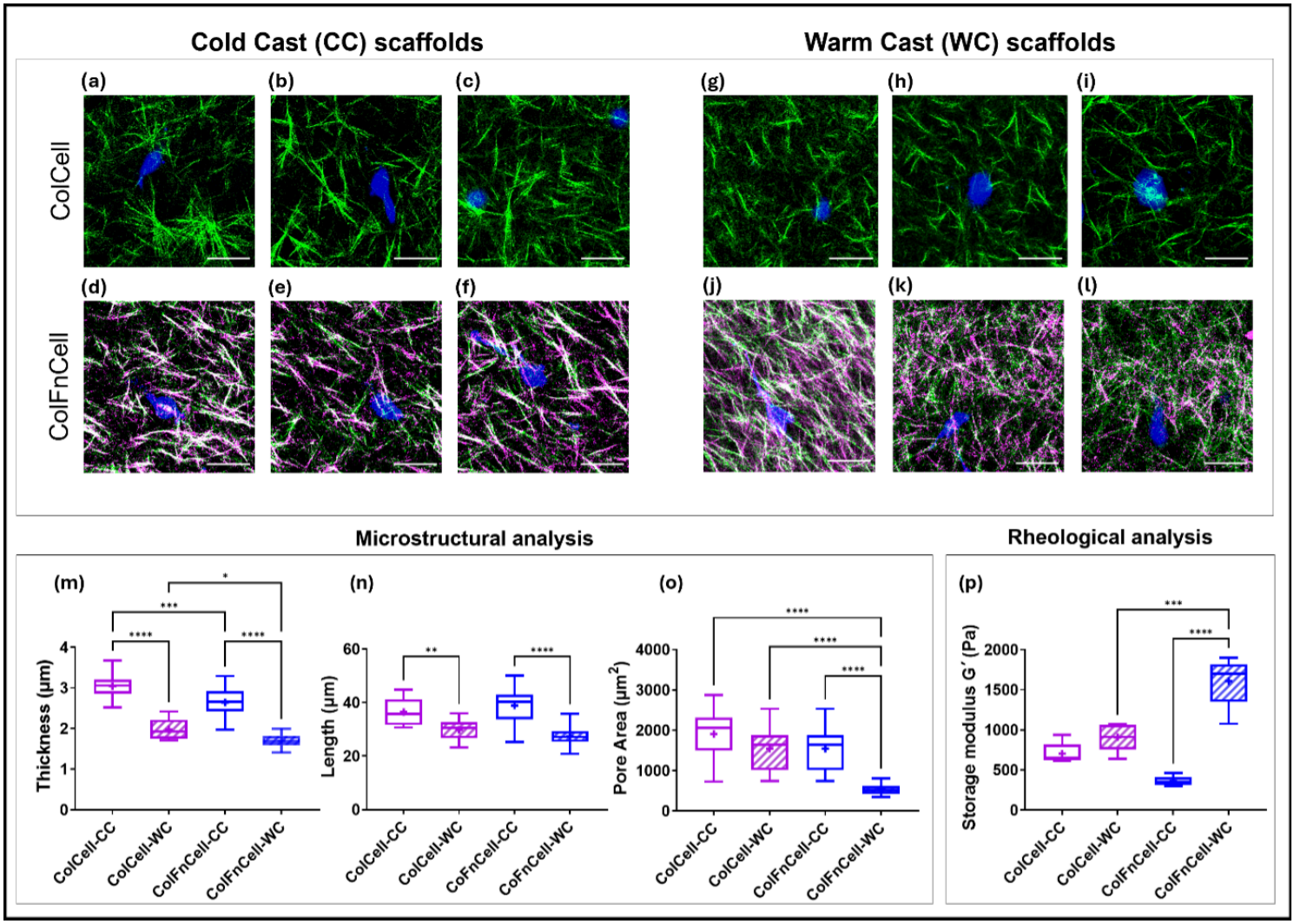


Figure 3

Fibronectin is required for cells to alter scaffold mechanics. (a–c) Cold-cast collagen-cell scaffolds (without fibronectin). (d–f) Cold-cast collagen-fibronectin-cell scaffolds. (g–i) Warm-cast collagen-cell scaffolds (without fibronectin). (j–l) Warm-cast collagen-fibronectin-cell scaffolds. Green: collagen reflectance; magenta: fibronectin fluorescence. Cells appear as non-fluorescent regions within the matrix. Scale bars: 50 µm. (m) Fibre diameter. (n) Fibre length. (o) Pore/mesh area. (p) Storage modulus revealing the key finding: in the presence of fibronectin, cells induce softening in cold-cast scaffolds but stiffening in warm-cast scaffolds, demonstrating bidirectional elasticity changes dependent on matrix microarchitecture. Data are presented as mean ± SD; n = 15 for structural analyses, n = 4 for rheological measurements. Statistical comparisons by one-way ANOVA with Tukey's post-hoc test; *$p < 0.05$, **$p < 0.01$, ***$p < 0.001$, ****$p < 0.0001$.

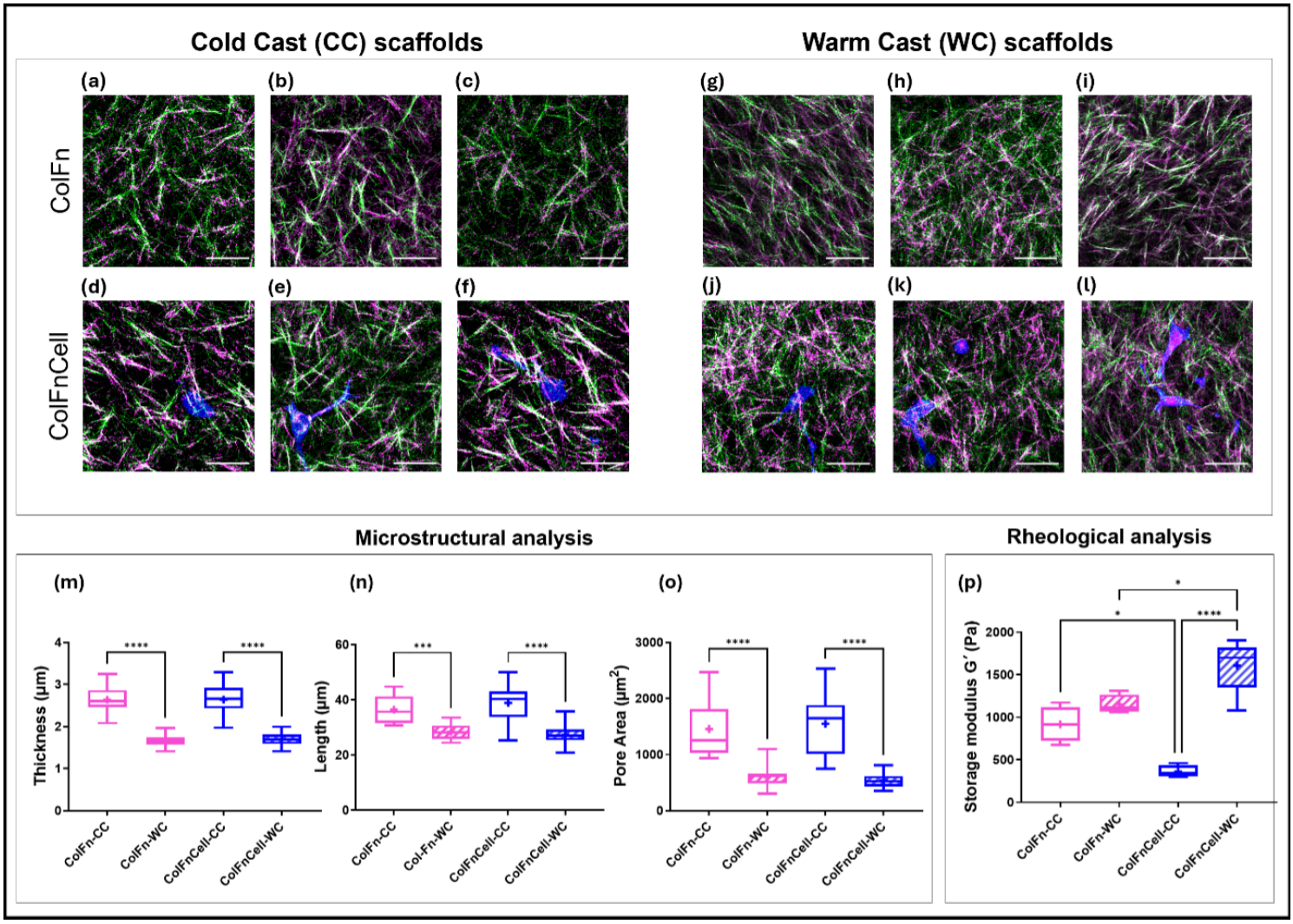


Figure 4

Direct comparison of cell-induced elasticity changes in collagen-fibronectin scaffolds with different microarchitectures. (a–c) Cold-cast collagen-fibronectin scaffolds without cells (control). (d–f) Cold-cast collagen-fibronectin-cell scaffolds showing cell-induced structural changes. (g–i) Warm-cast collagen-fibronectin scaffolds without cells (control). (j–l) Warm-cast collagen-fibronectin-cell scaffolds. Scale bars: 50 µm. (m) Fibre diameter. (n) Fibre length. (o) Pore/mesh area. (p) Storage modulus quantifying the magnitude of cell-induced elasticity changes: cells decrease stiffness by approximately 60% in cold-cast scaffolds while increasing stiffness by approximately 40% in warm-cast scaffolds. Data are presented as mean ± SD; n = 15 for structural analyses, n = 4 for rheological measurements. Statistical comparisons by one-way ANOVA with Tukey's post-hoc test; *$p < 0.05$, **$p < 0.01$, ***$p < 0.001$, ****$p < 0.0001$.

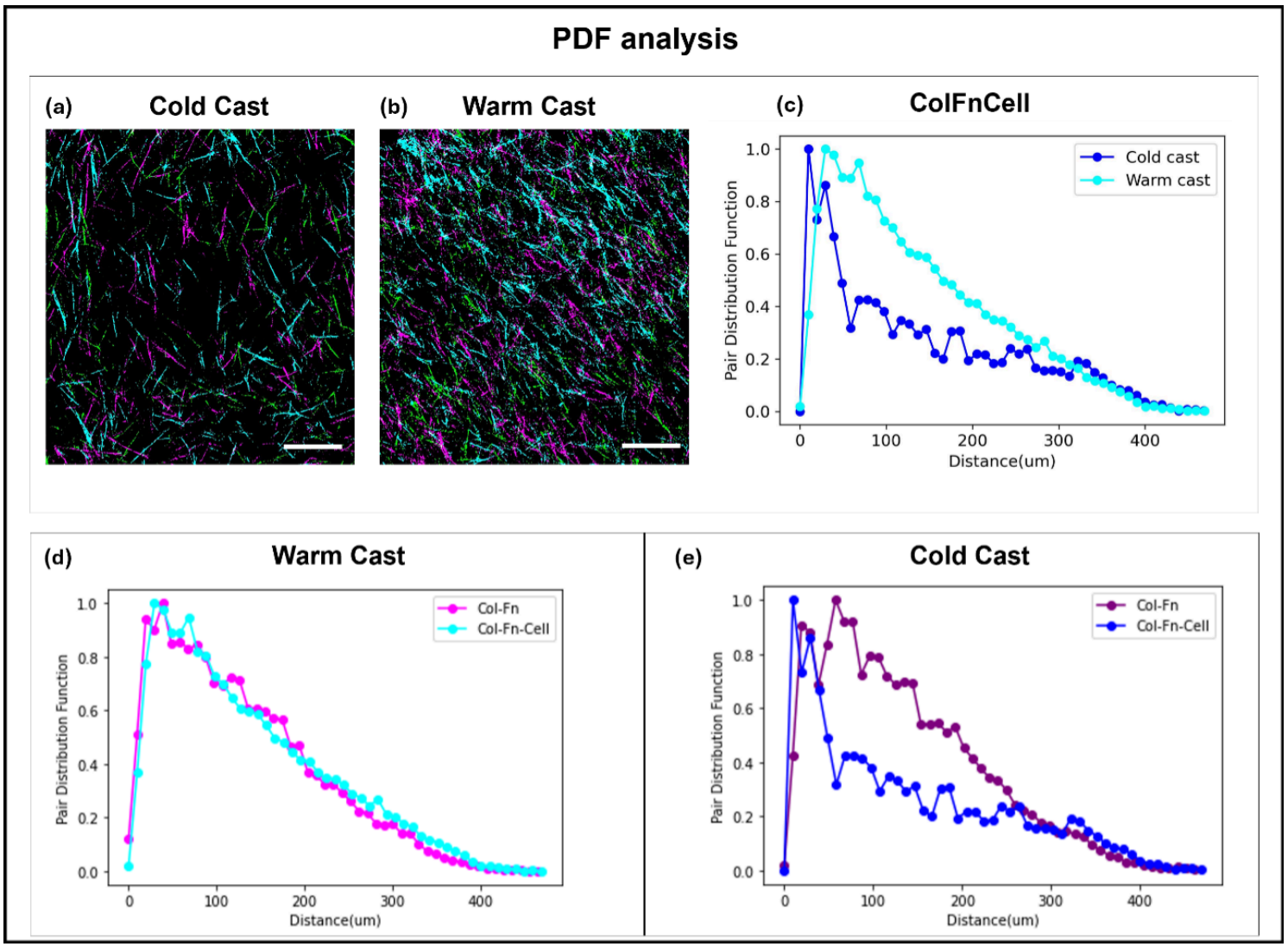


Figure 5

Pair distribution function analysis reveals distinct fibre spatial organisation in cell-laden scaffolds. (a) Representative pseudo-coloured confocal micrograph of cell-laden cold-cast collagen-fibronectin scaffold with three consecutive z-slices overlaid (cyan: layer 1; green: layer 2; magenta: layer 3). (b) Representative micrograph of cell-laden warm-cast scaffold processed identically. Scale bars: 100 μm. (c) Normalised pair distribution function (PDF) comparing fibre spatial organisation in cold-cast (blue) and warm-cast (cyan) cell-laden scaffolds. The biphasic decay in cold-cast scaffolds indicates reduced fibre connectivity and heterogeneous network structure. The near-linear decay in warm-cast scaffolds reflects maintained network organisation. (d) PDF comparison for warm-cast scaffolds with (ColFnCell, cyan) and without (ColFn, magenta) cells, showing minimal change in fibre distribution upon cell incorporation. (e) PDF comparison for cold-cast scaffolds with (ColFnCell, blue) and without (ColFn, purple) cells, demonstrating substantial alteration of fibre distribution in the presence of cells. These structural differences provide a basis for understanding the opposing elasticity changes observed in Figs. 3 and 4.

Supplementary Files

This is a list of supplementary files associated with this preprint. Click to download.

- SupplementaryInformationEslamietalnpjBiologicalPhysicsandMechanics.pdf